Stochastic Approximation to Reconstruction of Vector-Valued Images

Dariusz Borkowski

Abstract. In this paper we present a new method of reconstruction of vector-valued images with additive Gaussian noise. In order to solve this inverse problem we use stochastic differential equations with reflecting boundary. The reconstruction algorithm is based on Euler's approximations of solutions of such equations. We consider Euler scheme with random terminal time and controlled parameter of diffusion which is driven by geometry of $\mathbf{R}^n$- valued noisy image. Our numerical experiments show that the new approach gives very good results and compares favourably with deterministic partial differential equation methods.

1 Introduction

Let D be a bounded, convex domain in $\mathbf{R}^2$, $u : \overline{D} \to \mathbf{R}^n$ be an original image and $u_0 : \overline{D} \to \mathbf{R}^n$ be the observed image of the form $u_0 = u + \eta$, where η stands for a white Gaussian noise (added independently to all coordinates). We assume that u and u_0 are appropriately regular. We are given u_0, the problem is to reconstruct u. This is a typical example of an inverse problem [1].

Stochastic methods of image reconstruction are generally based on the Markov field theory, however some papers [3, 4, 7, 13, 14] involve advanced tools of stochastic analysis such as stochastic differential equations. The weakest point of this approach in the case of image denoising is the necessity of using Monte Carlo method. In particular, we have to do multiple simulations of trajectories of the diffusion process. Euler's approximation [11] is a classical method of diffusion simulations. This scheme gives good results only for small time-step discretization, but unfortunately reconstruction takes a very long time. In [3] the Euler scheme was improved for applications to image processing by adding a controlled parameter. This new

Dariusz Borkowski
Faculty of Mathematics and Computer Science, Nicolaus Copernicus University,
Chopina 12/18, 87-100 Toruń, Poland
e-mail: `dbor@mat.umk.pl`

R. Burduk et al. (Eds.): *CORES 2013*, AISC 226, pp. 393–402.
DOI: 10.1007/978-3-319-00969-8_38

numerical scheme considered for a constant terminal time T is called a modified diffusion (in short MD) and gives good results for long time-step discretization and reconstruction is about 50 times faster than with the Euler's approximation. In [4] the authors introduced a numerical scheme based on Euler's approximations with random terminal time. They considered the modified diffusion method with terminal time which depends on the geometry of the reconstructed image and therefore it is random. These modifications of the classical Euler scheme lead to the algorithm of denoising gray level images: modified diffusion with random terminal time (in short MDRTT), which compares favourably with modified diffusion method [3] and other classical denoising PDE filters.

A novel look in [4] on the reconstruction problem with the use of stochastic Euler approximation was fruitful and gave encouraging results for gray level images. The idea of this paper is to generalize these results to images with values in $\mathbf{R}^n$, in particular to colour images.

2 Mathematical Preliminaries

The reconstruction of images is based on two advanced tools of stochastic analysis: stochastic differential equations (in order to model image diffusion) and Skorokhod problem (in order to constrain the diffusion to image domain).

First we will define the Skorokhod problem. Let $D \subset \mathbf{R}^n$ be a domain with closure $\overline{D}$ and boundary ∂D. Let $T > 0$ and by $\mathbf{C}([0,T];\mathbf{R}^n)$ we denote a set of continuous functions $f : [0,T] \to \mathbf{R}^n$.

Definition 1. Let $y \in \mathbf{C}([0,T];\mathbf{R}^n)$, $y_0 \in \overline{D}$. A pair $(x,k) \in \mathbf{C}([0,T];\mathbf{R}^{2n})$ is said to be a solution to the Skorokhod problem associated with y and D if

1. $x_t = y_t + k_t, \;\; t \in [0,T]$,
2. $x_t \in \overline{D}, \;\; t \in [0,T]$,
3. k is a function with bounded variation $|k|$ on $[0,T]$, $k_0 = 0$ and

$$k_t = \int_0^t n_s \, d|k|_s, \; |k|_t = \int_0^t 1_{\{x_s \in \partial D\}} \, d|k|_s, \;\; t \in [0,T],$$

where $n_s = n(x_s)$ is an inward normal unit vector at $x_s \in \partial D$.

It is known that if D is a convex set, then there exists a unique solution to the Skorokhod problem [12].

Definition 2. Let $(\Omega, \mathscr{F}, \mathscr{P})$ be a probability space.

1. An n-dimensional stochastic process $X = \{X_t; t \in [0,T]\}$ is a parametrised collection of random variables defined on a probability space $(\Omega, \mathscr{F}, \mathscr{P})$ with values in $\mathbf{R}^n$.
   For each fixed $\omega \in \Omega$ the function $X_t(\omega)$, $t \in [0,T]$ is called a trajectory of X and is denoted by $X(\omega)$.

2. A filtration $(\mathscr{F}_t) = \{\mathscr{F}_t; t \in [0,T]\}$ is a nondecreasing family of sub-σ-fields of $\mathscr{F}$, i.e. $\mathscr{F}_s \subseteq \mathscr{F}_t \subseteq \mathscr{F}$ for $0 \leq s < t \leq T$.
   By $(\mathscr{F}_t^X)$ we denote a filtration generated by process X, i.e.
   $\mathscr{F}_t^X = \sigma(X_s; 0 \leq s \leq t)$.
3. A stochastic process X is adapted to the filtration $(\mathscr{F}_t)$ (X is $(\mathscr{F}_t)$ adapted) if for each $t \in [0,T]$, X_t is a $\mathscr{F}_t$ - measurable random variable.

Definition 3. Let Y be $(\mathscr{F}_t)$ adapted process with continuous trajectories, $Y_0 \in \overline{D}$. We say that a pair (X,K) of $(\mathscr{F}_t)$ adapted processes is a solution to the Skorokhod problem associated with Y and D, if for almost every $\omega \in \Omega$, $(X(\omega), K(\omega))$ is a solution to the Skorokhod problem associated with $Y(\omega)$ and D.

In what follows, by $W = \{W_t; t \in [0,T]\}$ we shall denote a Wiener process starting from zero. We assume that we are given a point $x_0 \in \overline{D}$ and some function $\sigma : \mathbf{R}^n \to \mathbf{R}^n \times \mathbf{R}^m$.

Definition 4. Let Y be an $(\mathscr{F}_t)$ adapted process. A pair $(X, K^{\overline{D}})$ of $(\mathscr{F}_t)$ adapted processes is called a solution to reflected SDE

$$X_t = x_0 + \int_0^t \sigma(X_s)\, dW_s + K_t^{\overline{D}}, \;\; t \in [0,T], \tag{1}$$

if $(X, K^{\overline{D}})$ is a solution to the Skorokhod problem associated with

$$Y_t = x_0 + \int_0^t \sigma(X_s)\, dW_s, \;\; t \in [0,T] \;\text{ and }\; D.$$

The process X is called the process with reflection. The proof of existence and uniqueness of the solution to reflected SDEs can be found in [12].

3 Reconstruction of Gray Level Images

We suppose for a while that the image is given by a function defined on the whole plane. Put $X_t = W_t^x$, $t \in [0,T]$, where W^x is a two-dimensional Wiener process starting from $x \in \overline{D}$. Then

$$\mathbf{E}[u_0(X_T)] = \int_{\mathbf{R}^2} \frac{1}{2\pi T} e^{-\frac{|x-y|^2}{2T}} u_0(y)\, dy = \int_{\mathbf{R}^2} G_{\sqrt{T}}(x-y) u_0(y)\, dy, \tag{2}$$

where $G_{\sqrt{T}}(x) = \frac{1}{2\pi T} e^{-\frac{|x|^2}{2T}}$ is a two-dimensional Gaussian mask.

The reconstructed pixel $u(x)$ is defined as the mean value $\mathbf{E}[u_0(X_T)]$. Therefore, by (2) the image is the convolution of the noise image with the two-dimensional Gaussian mask.

Since we want to consider the image as a function defined on the bounded convex set, we have to introduce a new assumption on the process X. It is natural to assume that the process X is a stochastic process with reflection with values in $\overline{D}$. In this case the process X is given by a Wiener process with reflection, i.e. it can be written as $X_t = W_t^x + K_t^{\overline{D}}$ (see Definition 4).

The above model removes noise and blurs edges. Following [8, 16] we provide a construction of an anisotropic diffusion model, where noise is removed and image has sharp edges. These conditions may be achieved by imposing

$$X_t = x + \int_0^t \begin{bmatrix} -\frac{(G_\gamma * u_0)_{x_2}(X_s)}{|\nabla(G_\gamma * u_0)(X_s)|}, & 0 \\ \frac{(G_\gamma * u_0)_{x_1}(X_s)}{|\nabla(G_\gamma * u_0)(X_s)|}, & 0 \end{bmatrix} dW_s + K_t^{\overline{D}}, \tag{3}$$

where $u_{x_i}(y) = \frac{\partial u}{\partial x_i}(y)$ and

$$u(x) = \mathbf{E}\left[u_0(X_T)\right].$$

To avoid false detections due to noise, u_0 is convolved with a Gaussian kernel $G_\gamma(x) = \frac{1}{2\pi\gamma^2} e^{-\frac{|x|^2}{2\gamma^2}}$ (in practice a 3×3 Gaussian mask).

3.1 Euler's Approximation

Consider the following numerical scheme

$$X_0^m = X_0, \; X_{t_k}^m = \Pi_{\overline{D}}[X_{t_{k-1}}^m + \sigma(X_{t_{k-1}}^m)(W_{t_k} - W_{t_{k-1}})], \; k = 1, 2, \ldots, m, \tag{4}$$

where $t_k = kh$, $h = \frac{T}{m}$, $k = 0, 1, \ldots, m$ and $\Pi_{\overline{D}}(x)$ denotes a projection of x on the set $\overline{D}$. Since D is convex, the projection is unique.

Theorem 1. *Let $(X, K^{\overline{D}})$ be the solution to the reflected SDE (1). If there exists $C > 0$ such that $\|\sigma(x) - \sigma(y)\|^2 \le C|x-y|^2$, then*

$$\lim_{m \to +\infty} |X_T^m - X_T| = 0 \quad \text{almost surely.}$$

The proof of the above theorem can be found in [11].

3.2 Modified Diffusion

The numerical scheme (4) gives good results, but only with a small value of the time-step parameter $h = \frac{T}{m}$ (for example $h = 0.05$). Calculating the mean value using Monte Carlo method for small h is not effective and takes a long time. To omit this problem, we improve the scheme (4) by adding a controlled parameter p [3].

$$X_0^m = X_0,\ H_{t_k}^m = \Pi_{\overline{D}}[X_{t_{k-1}}^m + \sigma(X_{t_{k-1}}^m)(W_{t_k} - W_{t_{k-1}})],$$

$$X_{t_k}^m = \begin{cases} H_{t_k}^m, & \text{if } \Theta, \\ X_{t_{k-1}}^m, & \text{elsewhere,} \end{cases} \qquad k = 1,2,\dots,m, \tag{5}$$

where by Θ we mean the condition $|(G_\gamma * u_0)(H_{t_k}^m) - (G_\gamma * u_0)(X_{t_{k-1}}^m)| < p$.

Note that the parameter $p > 0$ guarantees that if the image exhibits a strong gradient then the process X^m diffuses as a process with small value of the parameter h and at locations where variations of the brightness are small, the process X^m can diffuse with a large value of h (for example $h = 4$).

For small h or $p = +\infty$ (in practice $p > 255$) the numerical scheme (5) is equivalent to the scheme (4).

3.3 Modified Diffusion with Random Terminal Time

At locations where gradient is large in all directions it is possible that condition Θ does not hold as many times as we would expect. To avoid this we propose the following modification [4]:

$$X_0^m = X_0,\ H_{t_k}^m = \Pi_{\overline{D}}[X_{t_{k-1}}^m + \sigma(X_{t_{k-1}}^m)(W_{t_k} - W_{t_{k-1}})],$$

$$X_{t_k}^m = \begin{cases} H_{t_k}^m, & \text{if } \Theta, \\ X_{t_{k-1}}^m, & \text{elsewhere,} \end{cases} \qquad k = 1,2,\dots,\tau_m, \tag{6}$$

where $\tau_m = \min\{k; k \geq m \text{ and } \Theta \text{ is true } m \text{ times}\}$.

Terminal time τ_m guarantees that the numerical simulation of the diffusion trajectory gives at least m values of $X_{t_k}^m$ which differ from the value in the previous step. Observe that the scheme (6) works well only if the model of the digital image $G_\gamma * u_0$ is continuous. In practice, we can use a linear interpolation to get the value of the image $G_\gamma * u_0$, for any point $x \in \overline{D}$.

4 Reconstruction of Vector-Valued Images

Now we concentrate on images with values in $\mathbf{R}^3$. A very common idea to restore vector-valued images is to use scalar diffusion on each channel of a noisy image. But one quickly notices that this scheme is useless, since each image channel evolves independently with different smoothing geometries. To avoid this blending effect, the regularization process has to be driven in a common and coherent way for all the vector image channels. In order to execute that we use Di Zenzo geometry [5, 6].

Let $u : D \to \mathbf{R}^3$ be a vector-valued image and $x \in D$ be fixed. Consider the function $F_x : V \to \mathbf{R}$, $F_x(v) = \left|\frac{\partial u}{\partial v}(x)\right|^2$, where $V = \{v \in \mathbf{R}^2; |v| = 1\}$. We are interested in finding the arguments $\theta_+(u,x), \theta_-(u,x)$ and corresponding values $\lambda_+(u,x) = F_x(\theta_+(u,x))$, $\lambda_-(u,x) = F_x(\theta_-(u,x))$ which maximize and minimize the function F_x, respectively.

Note that F_x can be rewritten as $F_x(v) = F_x([v_1,v_2]^T) = v^T \mathbf{G}(x)v$, where

$$\mathbf{G}(x) = \begin{bmatrix} \sum_{i=1}^{3}\left(\frac{\partial u_i}{\partial x_1}(x)\right)^2, & \sum_{i=1}^{3}\frac{\partial u_i}{\partial x_1}(x)\frac{\partial u_i}{\partial x_2}(x) \\ \sum_{i=1}^{3}\frac{\partial u_i}{\partial x_1}(x)\frac{\partial u_i}{\partial x_2}(x), & \sum_{i=1}^{3}\left(\frac{\partial u_i}{\partial x_2}(x)\right)^2 \end{bmatrix}.$$

The interesting point about $\mathbf{G}(x)$ is that its positive eigenvalues $\lambda_+(u,x)$, $\lambda_-(u,x)$ are the maximum and the minimum of F_x while the orthogonal eigenvectors $\theta_+(u,x)$ and $\theta_-(u,x)$ are the corresponding variation orientations.

Three different choices of vector gradient norms $N(u,x)$ have been proposed in the literature $N_1(u,x) = \sqrt{\lambda_+(u,x)}$, $N_2(u,x) = \sqrt{\lambda_+(u,x) - \lambda_-(u,x)}$, $N_3(u,x) = \sqrt{\lambda(u,x) + \lambda_-(u,x)}$. In presented examples we have used $N(u,x) = \sqrt{\lambda_+(u,x)}$ as a natural extension of the scalar gradient norm viewed as the value of maximum variations.

Replacing in equation (3) $|\nabla(u,x)|$ and $[u_{x_1}(x), u_{x_2}(x)]^T$ respectively by $N(x,u)$ and $\theta_+(u,x) = [\theta_+^1(u,x), \theta_+^2(u,x)]^T$ we obtain the following model of anisotropic diffusion for vector-valued images:

$$X_t = x + \int_0^t \begin{bmatrix} -\frac{\theta_+^1(G_\gamma * u_0, X_s)}{N((G_\gamma * u_0)(X_s))}, & 0 \\ \frac{\theta_+^2(G_\gamma * u_0, X_s)}{N((G_\gamma * u_0)(X_s))}, & 0 \end{bmatrix} dW_s + K_t^{\overline{D}}, \tag{7}$$

where

$$u(x) = \mathbf{E}\left[u_0(X_T)\right].$$

4.1 Vector-Valued Modified Diffusion with Random Terminal Time

Considering in condition Θ the L^2 norm we have the following numerical scheme for vector-valued images (in short VMDRTT):

$$X_0^m = X_0,\ H_{t_k}^m = \Pi_{\overline{D}}[X_{t_{k-1}}^m + \sigma(X_{t_{k-1}}^m)(W_{t_k} - W_{t_{k-1}})],$$

$$X_{t_k}^m = \begin{cases} H_{t_k}^m, & \text{if } \Theta, \\ X_{t_{k-1}}^m, & \text{elsewhere}, \end{cases} \qquad k = 1,2,\dots,\tau_m, \tag{8}$$

where

$$\sigma(X^m_{t_{k-1}}) = \begin{bmatrix} -\frac{\theta^1_+(G_\gamma * u_0, X^m_{t_{k-1}})}{N((G_\gamma * u_0)(X^m_{t_{k-1}}))}, & 0 \\ \frac{\theta^2_+(G_\gamma * u_0, X^m_{t_{k-1}})}{N((G_\gamma * u_0)(X^m_{t_{k-1}}))}, & 0 \end{bmatrix},$$

$\tau_m = \min\{k; k \geq m \text{ and } \Theta \text{ is true } m \text{ times}\}$ and by Θ we mean the condition

$$|(G_\gamma * u_0)(H^m_{t_k}) - (G_\gamma * u_0)(X^m_{t_{k-1}})| < p,$$

where $|(x_1, x_2, x_3)| = \sqrt{x_1^2 + x_2^2 + x_3^2}$.

The picture in Fig. 1 presents a comparison of reconstruction results received with using the classical Euler's approximation [11] with long and short time-step discretization and VMDRTT (8). Figures c) d) e) are results of the reconstruction with the same value of diffusion parameter T. The reconstruction time of VMDRTT

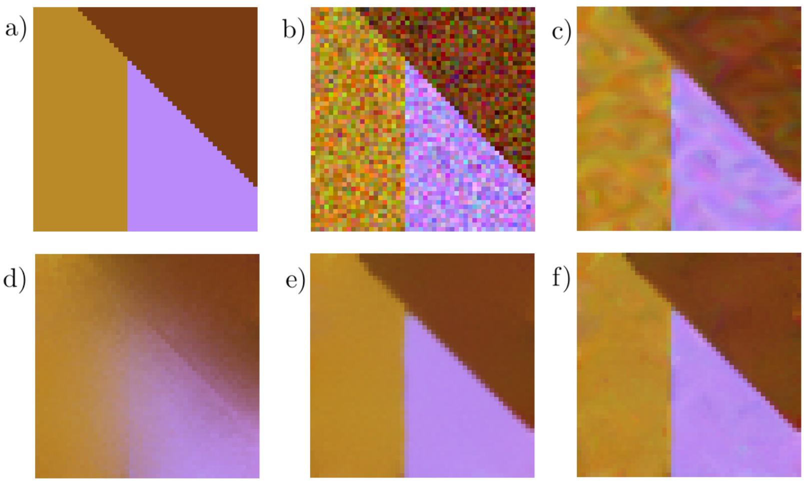

Fig. 1 a) Original image: 50×50 pixels b) Noisy image: standard deviation of the noise $\rho = 30$ c) Euler's scheme: $T = 56$, $h = 0.1$ (540 seconds) d) Euler's scheme: $T = 56$, $h = 4$ (13 seconds) e) VMDRTT: $T = 56$, $h = 4$ (16 seconds), $p = 30$ f) VMDRTT: $T = 16$, $h = 4$, $p = 30$ (5 seconds).

Table 1 SSIM

Standard deviation	$\rho = 20$	$\rho = 30$	$\rho = 40$
PM	0.8630	0.8105	0.7713
TV	0.8792	0.8335	0.7986
VMDRTT	0.8826	0.8438	0.8056

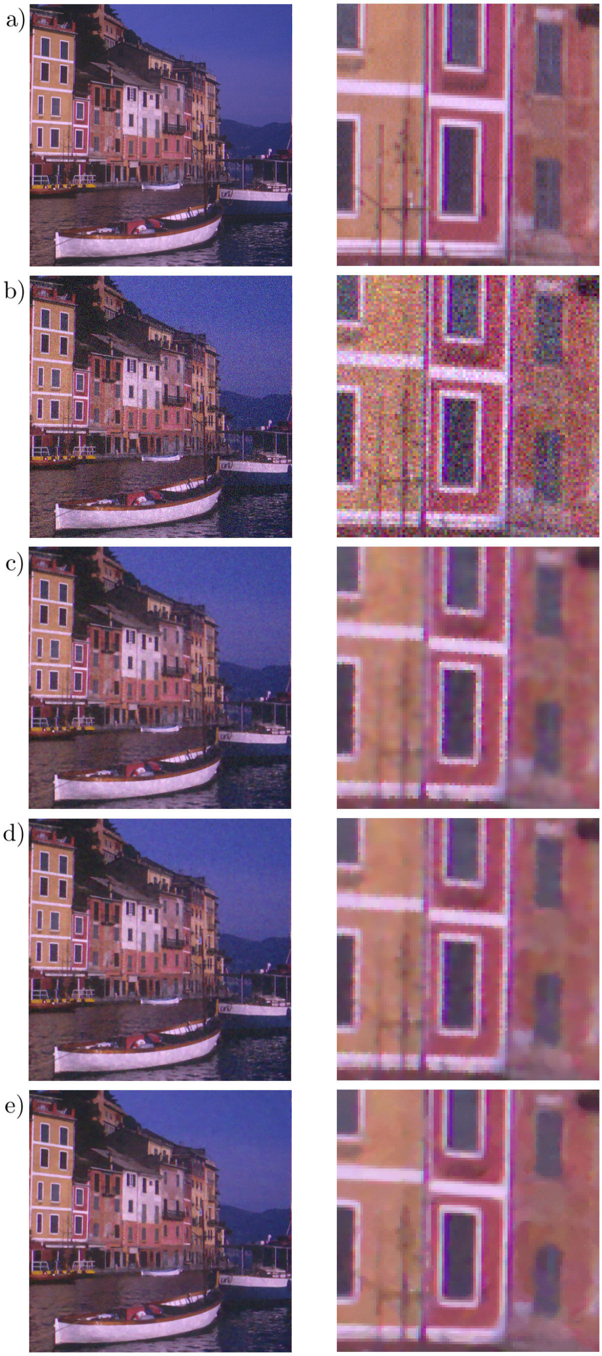

Fig. 2 a) Original image: 512×512 pixels b) Noisy image: $\rho = 20$ c) PM: SSIM=0.8630 d) TV: SSIM=0.8792 e) VMDRTT: SSIM=0.8826. Left: full images; right: a fragment chosen around the two windows surrounded by the darkest red wall.

was substantially reduced and the result is much better. The image c) is comparable to f) which is a result of VMDRTT with short diffusion parameter T. Note that we can obtain comparable results while reducing the time of the reconstraction by two orders – it is about 100 times faster.

5 Experimental Results

Some measures of quality for our evaluation experiments regarding VMDRTT and classic PDE methods: total variation [9] (in short TV) and Perona-Malik [8] (in short PM) for colour images [5, 10] are presented in Table 1 and Fig. 2. The results refer to RGB image *portofino* corrupted (channels independently) with the Gaussian noise with standard deviation ρ. Noisy images have been reconstructed with vector analysis in RGB space. The maximum values of Structural Similarity Index (in short SSIM) are given in the table. Definition of SSIM error in gray scale can be found in [15]. In order to count SSIM in RGB color space we apply SSIM measure to each individual color component and next we average the result [2]. Parameters of SSIM were set to the default values as recommended by [15].

When comparing the figures one can observe that the image created by the stochastic method is visually more pleasant. The reason for this is that PDE methods show clear evidence of a block image, but this stair-case effect is reduced in our algorithm. Moreover, an analysis of the measures of image quality shows that VMDRTT method performs better.

6 Conclusion

In this paper we have presented a new colour denoising method based on Euler's approximation of reflected SDEs. The obtained results demonstrate the efficiency of the proposed approach, compared with the classical Euler scheme.

References

1. Aubert, G., Kornprobst, P.: Mathematical problems in image processing. Springer, New York (2002)
2. Astrom, F., Felsberg, M., Lenz, R.: Color Persistent Anisotropic Diffusion of Images. In: Proceedings of the 17th Scandinavian Conference on Image analysis (SCIA), pp. 262–272 (2011)
3. Borkowski, D.: Modified diffusion to image denoising. Adv. Soft Comp. 45, 92–99 (2007)
4. Borkowski, D.: Euler's Approximations to Image Reconstruction. In: Bolc, L., Tadeusiewicz, R., Chmielewski, L.J., Wojciechowski, K. (eds.) ICCVG 2012. LNCS, vol. 7594, pp. 30–37. Springer, Heidelberg (2012)

5. Deriche, R., Tschumperlé, D.: Diffusion PDE's on vector-valued images: local approach and geometric viewpoint. IEEE Signal Processing Magazine 19(5), 16–25 (2002)
6. Di Zenzo, S.: A note on the gradient of a multi-image. Comput. Vis. Graph. Image Process. 33(1), 116–125 (1986)
7. Juan, O., Keriven, R., Postelnicu, G.: Stochastic Motion and the Level Set Method in Computer Vision: Stochastic Active Contours. Int. J. Comput. Vision 69(1), 7–25 (2006)
8. Perona, P., Malik, J.: Scale-space and edge detection using anisotropic diffusion. IEEE Trans. Pattern Anal. Mach. Intell. 12(7), 629–639 (1990)
9. Rudin, L.I., Osher, S., Fatemi, E.: Nonlinear total variation based noise removal algorithms. Physica D 60(1-4), 259–268 (1992)
10. Sapiro, G., Ringach, D.L.: Anisotropic diffusion of multivalued images with applications to color filtering. IEEE Trans. Image Process. 5(11), 1582–1585 (1996)
11. Słomiński, L.: Euler's approximations of solutions of SDEs with reflecting boundary. Stoch. Proc. Appl. 94, 317–337 (2001)
12. Tanaka, H.: Stochastic differential equations with reflecting boundary condition in convex regions. Hiroshima Math. J. 9(1), 163–177 (1979)
13. Unal, G., Krim, H., Yezzi, A.: Stochastic differential equations and geometric flows. IEEE Trans. Image Process. 11(12), 1405–1416 (2002)
14. Unal, G., Ben-Arous, G., Nain, D., Shimkin, N., Tannenbaum, A., Zeitouni, O.: Algorithms for stochastic approximations of curvature flows. In: Image Processing, Proceedings ICIP 2003, vol. 2-3, pp. 651–654 (2003)
15. Wang, Z., Bovik, A.C., Sheikh, H.R., Simoncelli, E.P.: Image quality assessment: From error visibility to structural similarity. IEEE Trans. Image Process. 13(4), 600–612 (2004)
16. Weickert, J.: Theoretical Foundations Of Anisotropic Diffusion In Image Processing. Computing Suppement 11, 221–236 (1996)